Table 1 Comparison of base pressure rises

Configuration	$\dot{m}_{fuel}/\rho_1 u_1 h$ Total	Base	Side	p_b/p_∞	p_1/p_∞	ℓ/h	f_s	$(T_0)_{throat}$	M_j
	0.213	0.213	...	1.08	1.00	69	0.383	2220	0.688
All base	0.162	0.162	...	1.05	1.00	78	0.256	2300	0.527
	0.050	0.050	...	0.87	1.00	73	0.81	2500	0.212
Combined base/*EB*	0.213	0.062	0.151	1.08	1.21	105	0.073	2500	0.227
All *EB*	0.023	...	0.023	0.51	1.21	16	0.073	...	...

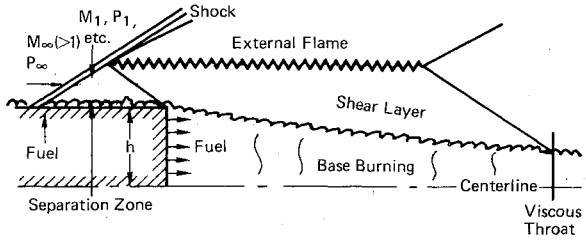

Fig. 1 Schematic of flowfield model with external burning.

with $k=0.01$. Again following our work for the base region, the entrained air has an effective heating value when combined with the fluid in the fuel-rich zone, so that

$$q=c_p\dot{m}\,dT_0=d\dot{m}\,[h_f f_s+c_p(T_{0_1}-T_0)] \tag{3}$$

If the first term in the brackets is much larger than the second, or if both terms are contained into an "effective" heating value $(h_f f_s)_{eff}$, then

$$q=\dot{m}_{air}\,(h_f f_s)_{eff}/\ell \tag{4}$$

where ℓ is the length of the flame. Finally

$$C_p=\frac{(\gamma-1)\;2k\,(h_f f_s)_{eff}}{(\gamma R T_1)\,(M_1^2-1)^{1/2}}\;\frac{\sin\mu}{\sin(\mu+\alpha)} \tag{5}$$

The minimum amount of fuel required to produce this situation can be back-calculated as follows. First, ℓ is found from the base-flow analysis such that the last wave from the external burning region strikes the base flow at the viscous throat. The air contained in this length equals

$$\dot{m}_{air}=2(k)\rho_1 u_1 \ell \tag{6}$$

so that the fuel required is

$$\dot{m}_{fuel}/\rho_1 u_1 h=\dot{m}_{air} f_s/\rho_1 u_1 h=2k\;f_s(\ell/h) \tag{7}$$

Results

Consider now a specific situation

$$M_\infty=2.3;\;T_{0_\infty}=T_{0_1}=1000°R;\;\gamma=1.4$$

$$(T_0)_{fuel}=1150°R;\;(\delta/h)<0.1;$$

and $$(h_f f_s/C_p)_{eff}=1600°R$$

with three different configurations: all base-burning, all external-burning (*EB*), and combined *EB*/base-burning. In Table 1, compare the first entry in the all-base situation with the combined *EB*-base case. They have the same total fuel flow and virtually the same base pressure level. The high *EB* fuel flow rate for the combined case is a direct result of the very long base flow region ($\ell/h=105$) predicted with substantial heat release and a low base injection rate. The fuel/air ratio f_s is obtained with the assertion that all of the fuel injected through the base is consumed by the viscous throat. Put another way, the mixture is fuel-rich or at least stoichiometric up until the viscous throat.

The results for the all-*EB* case are particularly informative: the base region is short ($\ell/h=16$), so that the required fuel flow [see Eq. (7)] and resultant p_b/p_∞ are low. Increasing the fuel flow rate for this case beyond the level shown will not increase p_b, since air will not be available for combustion until beyond the point where *EB* can effect the base flow ahead of the viscous throat and change p_b. Higher p_b might be achieved, however, by stacking (or staggering injectors with the initial compression wave of each flame sheet intersecting the corner of the base), increasing the air entrainment rate, and assuming discrete-hole injection instead of an injection sheet.

References

[1]Strahle, W. C., "Theoretical Considerations of Combustion Effects on Base Pressure in Supersonic Flight," *Twelfth International Symposium on Combustion*, 1968 Poitiers, France.

[2]Schetz, J. A., Billig, F. S., and Favin, S., "Simplified Analysis of Supersonic Base Flows Including Injection and Combustion," *AIAA Journal*, Vol. 14, Jan. 1976, pp. 7-8.

[3]Tsien, H. S. and Beilock, M., "Heat Source in a Uniform Flow," *Journal of Aeronautical Science*, Dec. 1949, p. 756.

Pit Formation on the Accelerated Solid Propellant Combustion Surface

Tohru Mitani*
National Aerospace Laboratory, Miyagi, Japan

Introduction

IT has been reported that the burning rate of solid propellants increases in the acceleration field. This phenomenon is caused by the local burning rate increases (pit formation) by agglomerated aluminum spheres on the accelerated combustion surface. Many experimental and analytical studies have been carried out regarding this acceleration-induced burning rate increase of solid propellants. But all of the studies are concerned with the mechanism of local heat feedback on each pit, not with the density or distribution of pits themselves. Up to the present time, no detailed investigation except a paper by Niioka, et al.[1] has been published concerning the pitting phenomenon on the accelerated combustion surface. In order to clarify the acceleration sensitivity of solid propellants, however, it is necessary to study the pitting mechanism. This is because the pitting mechanism determines the transient period of combustion[2,3] the instantaneous

Received April 19, 1976; revision received May 19, 1976.
Index categories: Combustion in Heterogeneous Media; Fuels and Propellants, Properties of.

*Research Engineer, Kakuda Branch.

burning rate, and the time-averaged burning rate of solid propellants in an acceleration environment.

This paper is concerned with slab motor experiments conducted to study the pit density on the accelerated combustion surfaces for aluminized and nonaluminized composite propellants. The effects of burning pressure, acceleration level, and addition of aluminum powder on the density will be discussed.

Propellants and Experimental Method

Two CTPB (corboxy terminated polybutadiene)-AP (ammonium perchlorate)-Al (aluminum) propellants and a CTPB-AP propellant were used for this study. PB05 aluminized propellant with 8.2% aluminum and PB04 nonaluminized propellant were used to investigate the effects on the pitting by aluminum particles and ammonium perchlorate particles, respectively. The combined effect of aluminum and ammonium perchlorate particles was studied by using PB10 aluminized propellant containing 2.0% aluminum. Aluminum powder for aluminized propellants has a particle distribution with a mass median diameter ($\bar{d}$) of 48μ and a log normal distribution variance (σ) of 0.696.

The 50 × 100-mm combustion surface and 15-mm thick propellant slabs were fired with the acceleration field being directed toward the combustion surface up to 100g and with a burning pressure of 20 ~ 70 kg/cm^2. In order to observe the accelerated combustion surfaces, their combustion was extinguished at given times from 0.3 to 1.0 sec after ignition. These extinction tests were done by means of rapid depressurization and injection of water. From the extinguished combustion surfaces, the pit density (N_p), the number of pits per unit combustion surface area, was calculated, and the effects of acceleration, burning pressure, and propellants on it were investigated.

Results and Discussion

The burning pressure and acceleration dependence of pit density at the extinction time of 0.33 sec is shown in Fig. 1. The pit density increases as the acceleration level or the burning pressure increases. In order to explain this dependency, it is necessary to consider the agglomeration rate of aluminum particles, because the pits on the accelerated combustion surface are formed by agglomerated aluminum spheres. The evolution of agglomerated aluminum spheres depends on the collision of aluminum particles released from the combustion surface, although the agglomeration mechanism in an acceleration environment seems to be different from its counterpart in a nonacceleration environment. This is because aluminum particles with strong body forces move in a complex manner, and they stay in the neighborhood of the combustion surface.[4] The agglomeration mechanism in such an environment can be considered as follows.

The aluminum particles retained by acceleration burn in a lower temperature region above the combustion surface, and they are blown away when they become smaller than the critical particle size determined by means of the Stokes' law on drag. On the other hand, the collision rate of particles is proportional to the number of particles per unit volume. So, it is reasonable to assume that the collision rate in an acceleration environment is proportional to the supply rate of aluminum particles into a unit volume of the lower temperature region between the combustion surface and the flame. The number of retained aluminum particles, which have been released per unit combustion surface area, can be written as

$$\frac{\rho_{\text{prop}} r_0 wG}{(\pi/6)\rho_{\text{al}} d_l^3} \tag{1}$$

where d_l is the diameter of retained aluminum particles, G the retained rate of aluminum particles, ρ the density, r_0 the static

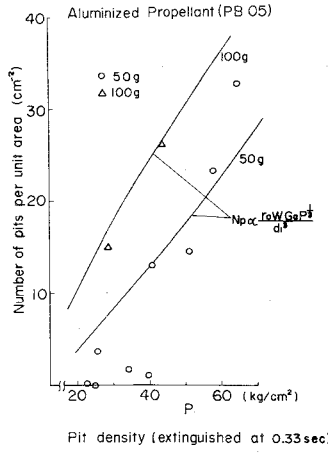

Fig. 1 Effect of pressure and acceleration on pit density (extinguished at 0.33 sec).

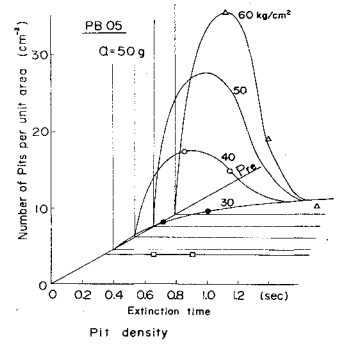

Fig. 2 Effect of pressure and burning time on pit density (acceleration α = 50g).

burning rate of the propellant and w the weight fraction of aluminum in the propellant; subscripts (al) and (prop) represent aluminum and propellant, respectively. Postulating a log normal distribution with a mass median diameter ($\bar{d}$) and a variance (σ) for the contained aluminum particles and using a critical diameter for retained particles (d_0) yield the retained rate of aluminum (G)

$$G = \tfrac{1}{2}\text{erfc}\{\ln(d_0/\bar{d})/\sigma\} \tag{2}$$

The d_0 can be estimated by Stokes' law for drag as follows;

$$d_0 = \left\{\frac{18 r_0 \rho_{\text{prop}} (1-w)\mu_g}{\rho_g \rho_{\text{al}} \alpha}\right\}^{1/2} \tag{3}$$

where α is acceleration level, μ the viscosity, and subscript (g) represents gases. If one assumes that the diameters of retained aluminum particles (d_l) can be represented by a diameter giving a half retained rate of aluminum, it is given by

$$\tfrac{1}{2}G = \tfrac{1}{2}\text{erfc}\{\ln(d_l/\bar{d})/\sigma\} \tag{4}$$

The lower temperature region accumulating the aluminum particles can be represented by the standoff distance of flame, which varies with $P^{-1/3}$ for composite propellants, where P is the burning pressure. As a result, the pit density (N_p) can be expressed as

$$N_p = C\frac{\rho_{\text{prop}} r_0 wG}{d_l^3} P^{1/3} \tag{5}$$

where C is an empirical constant of pit formation. This relationship shown in Fig. 1 gives the strong pressure and acceleration dependence of pit density, and the curves using a C value of 1.2 × 10^{-5} almost coincide with experimental results except in the low pressure region.

Figure 2 illustrates the effects on the density of burning time and burning pressure with acceleration value (50g) as a

parameter. It shows that pit density increases with the burning time in a low burning pressure region, but in a high burning pressure region it increases to a maximum value and then decreases due to the agglomeration of neighboring pits (or convergence) with time. Regarding the effect of burning pressure, the pit density increases enormously with pressure during the initial burning time (0~0.4 sec). In the second stage, however, where burning time is longer (0.4 sec~), the high burning pressure leads to the high rate of convergence of pits, so that the pit density in a high pressure region becomes lower than that in a low burning pressure region.

In regard to pit formation, there is a critical pressure of about 25kg/cm^2 which is not affected by acceleration level, burning time, or the propellants used for this investigation. Although no pits exist on extinguished combustion surfaces below the critical pressure, many agglomerated spheres are observed on them. Therefore, it is necessary to consider another factor for pitting of accelerated combustion surface in addition to the agglomeration of retained aluminum particles. It has been reported that there is a critical relationship between pit density and acceleration level, and that the agglomerated aluminum spheres cannot promote the burning rate of the propellant under a critical value of acceleration.[5,6] Thus, it seems that there is an analogous mechanism to the burning pressure, and the phenomenon will be explained through the lift distance increase of the spheres by decreasing pressure, which causes the reduction of the amount of heat feedback to combustion surface.

Many discrete pits with sharp bottoms also can be seen on the extinguished combustion surfaces of PB04 nonaluminized propellant, which are made by AP particles contained in the propellant. The PB04 propellant has a lower pit density in the low acceleration field, and a higher pit density in the high acceleration field in comparison with the aluminized propellant PB05. But this high pit density by AP particles does not always yield high acceleration sensitivity of the burning rate of aluminized propellants. That is, the result of the PB10 propellant containing 2.0% aluminum shows that the extinguished combustion surfaces are covered by continuous round-bottomed pits which are characteristic of pits formed by agglomerated aluminum spheres. Thus, it is concluded that aluminum particles have a dominant role in the pitting at the initial burning time, and the pitting by AP particles need not be considered for high-aluminized composite propellants.

Conclusions

Extinction tests of slab motors were conducted to investigate the pitting on the accelerated combustion surface responsible for the acceleration-induced burning rate increase. A pit density chart on the burning pressure and the burning time with acceleration as a parameter was obtained for an aluminized propellant. It shows that pit density increases with the acceleration and the burning pressure initially, but that it decreases with burning time after reaching a maximum value in high burning pressure region. This decrease of pit density is due to the convergence of neighboring pits, which can be distinguished by the shape of continuous shallow pits on the extinguished combustion surfaces. The initial strong pressure dependence can be explained by formulating the accumulation rate of retained aluminum particles on the accelerated combustion surface. For all propellants used, there was a critical burning pressure of 25kg/cm^2, and no pits were observed on the combustion surfaces below this value. This critical pressure may be explained through the heat feedback mechanism by the agglomerated aluminum sphere. It was shown by using a nonaluminized propellant that AP particles also had the potential to form many pits on the accelerated combustion surfaces. These pits, however, need not be considered except in the case of non/low-aluminized propellants, because of the dominant effect of aluminum particles on pit formation.

References

[1] Niioka, T., Mitani, T., and Ishii, S., "Observation of the Combustion Surface by Extinction Tests of Spinning Solid Propellant Rocket Motors," *Proceedings of the 11th International Symposium of Space Technology and Science,* 1975, pp. 77-82.

[2] Northam, G. B., "Effects of the Acceleration Vector on Transient Burning Rate of an Aluminized Solid Propellant," *Journal of Spacecraft and Rockets,* Vol. 8, Nov. 1971, pp. 1133-1137.

[3] Niioka, T., Mitani, T., and Ishii, S., "Transient Period of the Acceleration-Produced Burning Rate Augmentation," *AIAA Journal,* Vol. 14, 1976, to be published.

[4] Doin, B., Brulard, J., and Larue, P., "Facilities for Studying the Combustion of Spinning Metallized Solid Propellants," TN-229, 1974, ONERA.

[5] Niioka, T. and Mitani, T., "Independent Region of Acceleration in Solid Propellant Combustion," *AIAA Journal,* Vol. 12, Dec. 1974, pp. 1759-1761.

[6] Mitani, T. and Niioka, T., "Firing Tests of Spinning 200ϕ-Solid Propellant Rocket Motors," *19th Symposium on Space Science and Technology,* Nagoya, Japan, 1975, pp. 201-204, in Japanese.

Technical Comments

Comment on "Application of Hamilton's Law of Varying Action"

Arthur E. Bryson Jr.
Stanford University, Stanford, Calif.

WE believe that the theory in Ref. 1 is basically incorrect. From Ref. (2) Hamilton's Principle for holomonic nonconservative systems may be stated as follows: the first variation of the time integral of system kinetic energy plus the time integral of system virtual work is zero, i.e.

$$\delta \int_{t_o}^{t_1} T(q_i, \dot{q}_i)\,dt + \int_{t_o}^{t_1} \sum_j Q_j(q_i, \dot{q}_i)\,\delta q_j\,dt = 0$$

where q_1, ---, q_n are the generalized coordinates, T is kinetic energy, Q_1, --- Q_n are generalized forces, and δ indicates an infinitesimal variation; $\sum_j Q_j\,\delta q_j$ is the virtual work, where the Q_j are defined by the fact that the work done on the system by the Q_j is given by the path-dependent line integral

$$W = \sum_j \int_{q_j(t_o)}^{q_j(t_1)} Q_j(q_i, \dot{q}_i)\,dq_j$$

Bailey claims that a variational principle for nonconservative systems is (cf. Eq. (4) of Ref. 1)

$$\delta \int_{t_o}^{t_1} (T+W)\,dt = \sum_j \frac{\partial T}{\partial \dot{q}_j}\delta q_j \,|\, t_o^{\,t}$$

but does not define the work W so that $\delta\int_{t_0}^{t_1} W dt$ is a meaningless expression. In his first example virtual work (instead of work) is used in Eq. (5). In his second example, in Eq. (11), work is incorrectly defined for the hinge moments of the double pendulum. The correct definitions are

Received Jan. 30, 1976.
Index category: Structural Dynamic Analysis.

*Professor and Chairman, Dept. of Aeronautics and Astronautics. Fellow AIAA.